F-band Millimeter-wave Signal Generation for Wireless Link Data Transmission Using On-chip Photonic Integrated Dual-wavelength Sources

Robinson Guzman[1], **Guillermo Carpintero**[1], **Carlos Gordon**[1], **Katarzyna Lawniczak**[2], **and Xaveer Leijtens**[2]

[1]Tecnología Electrónica, Universidad Carlos III de Madrid, Leganés, Madrid, Spain
[2]Photonic Integration, Technical University of Eindhoven, Eindhoven, The Netherlands

Abstract— Millimeter-waves (30–300 GHz) have interest due to the wide bandwidths available for carrying information, enabling broadband wireless communications. Photonics is a key technology for millimeter wave signal generation, recently demonstrating the use of photonic integration to reduce size and cost. In this paper, we present two dual-wavelength Photonic Integrated Circuit (PIC) structures designed for signal generation using the optical heterodyne technique. We demonstrate a 1 Gbps data rate wireless link that does not require any stabilization scheme to lock the two wavelengths. Both integrated dual-wavelength sources are based on an Arrayed Waveguide Grating element. A novel building block -Multimode Interference Reflectors (MIRs) — is used to integrate on-chip one of these structures, without need of cleaved facets to define the laser cavity. This fact enables us to locate any of these structures at any location within the photonic chip.

1. INTRODUCTION

Generation of signals with frequencies in the upper millimeter-wave (mmW) band (> 60 GHz) has recently become attractive. This frequency band has a wide range of potential applications from broadband wireless communications, Radio-over-Fiber (RoF) to spectroscopy [1]. In broadband wireless communications, the use of higher mmW carrier frequencies is a cost-effective method that allows increasing the data rate using simple modulation formats as ON-OFF Keying (OOK) or Amplitude Shift Keying (ASK). This avoids costly computational coding schemes. The broad available bandwidth gives these ranges the potential to become key in the convergence between wired (fiber optic networks) and wireless (backhauling 5G) services. Among the obstacles to develop millimeter wave applications is the lack of signal sources [2]. The generation of signals above 100 GHz is challenging using full-electronic techniques [3]. Photonic techniques are considered to be superior providing wide bandwidth, broad tuning range and superior stability.

There are several photonic techniques that are available for mmW generation. Among the different optical signal generation techniques, optical heterodyning is the most promising. This method requires an optical signal source generating two different wavelengths that are mixed into a photodiode or photoconductor (used as photomixer) [4]. The generated signal is an electrical beat-note at a frequency given by the difference between the wavelengths. Photonic integration advances have already been reported in this line [5]. Photonic Integrated Circuits (PIC) have key advantages enabling the integration of multiple photonic building blocks within a single chip, increasing compactness, functionality and performance [5]. Integration reduces fiber coupling interfaces having a huge impact on the cost and component footprint, allowing compact and cost efficient mmW transmitters.

In this work we present a photonic-based millimeter-wave signal source using monolithically integrated dual-wavelength sources based on arrayed waveguide grating (AWG) using a new building block, Multimode Interference reflectors (MIR) [7]. The main advantage of this approach is that we do not require the chip facets for the laser resonator, enabling on-chip post-processing of the dual wavelength signal. In addition, samples were fabricated using a multi-project wafer (MPW) run under a generic technology foundry, which further addresses cost issues. Furthermore, this paper presents our progress in F-band wireless link system technologies that contribute to extending the transmission distance of the wireless links.

2. DUAL-WAVELENGTH LASER SOURCES

Two different structures of monolithically integrated dual-wavelength laser sources (DWLS) have been developed which are suitable for fabrication in a Generic InP-based technology platform through a Multi-Project Wafer (MPW) run. The first DWLS consists of a set of sixteen SOAs, one per channel, labeled CH N (with $N = 1$ to 16), as shown in Fig. 1(a). All the SOAs used for the channel selection are 600 µm long. An additional SOA is located at the AWG's common output in order to boost the output optical power of the two wavelengths generated by two separated channel biased simultaneously. The length of the Boost amplifier is 750 µm. The AWG central wavelength is $\lambda = 1550$ nm, the channel spacing $\Delta\lambda = 0.8$ nm (100 GHz) and the FSR is 7.2 nm (900 GHz). The frequency spacing between the two generated wavelengths is an integer multiple of the AWG channel spacing ($\Delta\lambda$). A drawback of this structure is that the wavelength spacing is not tunable since it is fixed by the AWG.

The novelty of our design is that is an on-chip solution through the use of novel multimode interference reflectors (MIR), shown in Fig. 1(c) to create the required Fabry-Perot cavity of the AWG laser without requiring the facets of the chip which has been implemented and developed on the second DWLS. This device consists of an AWG with 4 channels, one SOA per channel labeled SOA N (with $N = 1$ to 4) and one common output, as shown in Fig. 1(b). Two of the channels implement EOPMs. The designed AWG has a $\Delta\lambda$ and a FSR of 0.961 nm (120 GHz) and 5.61 nm (700 GHz), respectively. All the SOAs used both for the channel selection and for the common output are 400 µm long. The lengths of the EOPMs are 1000 µm. MIR reflector structures implemented in this design derive from a standard multimode interference (MMI) coupler, in which deeply etched 45 mirrors at suitable locations reflect back the light by total internal reflection.

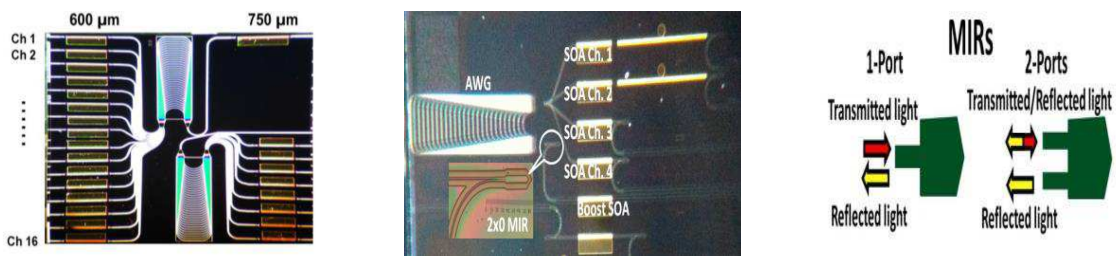

(a) (b) (c)

Figure 1: (a) Microscope photograph of cleaved facet structure 16-channels AWGL. The cleaved facets of the chip use as mirror a partially reflective (PR) coated with a reflection value of 32% approximately. (b) Microscope photograph of on-chip structure 4-channels AWG , two of them with EOPM and two other without. MIRs are used to define the FP cavity, and one Boost amplifier at the CO. MIRs' reflectivity has a value about 60%. (c) 1-port (left) and 2-ports (right) MIRs.

3. PHOTONIC WIRELESS LINK DATA TRANSMISSION SYSTEM

This section describes an F-Band (90–140 GHz) wireless data transmission link using the PICs described above as signal sources at the transmitter, with on-off keying (OOK) modulation format and envelope detection at the receiver. In Fig. 2(a), a schematic diagram of the experimental setup where the photonic technique of optical heterodyning is employed for the generation and modulation of mmW signals is shown. A photograph of the photonic wireless link data transmission system measurement setup is shown in Fig. 2(b). A guide rail with a length about 30 cm is used for moving the SBD away from the transmitter, from 0 cm to 24 cm. For evaluating the bit error rate measurement at different distances between the transmitter and receiver, the average output power generated by the U2T PIN photodiode (PD) is set at 2.4±0.35 mW for 101 GHz and 0.87±0.15 mW for 114 GHz carrier frequency, respectively. The average input optical power of the PIN-PD is set at 10.5 dBm. A difference of 5 dBm between 101 GHz and 114 GHz carrier frequency at the PIN-PD's output is obtained due to the fact that the −3 dB cutoff frequency of the PIN-PD is about 95 GHz, thus take this value into account is very important for the analysis of the BER measurement of the wireless link.

In Fig. 3(a) and Fig. 4(a) are shown eye pattern demodulated, amplified and filtered by the receiver module with a wireless carrier frequency of 101 GHz and 114 GHz, respectively. Likewise, in Fig. 3(b) and Fig. 4(b) are shown the bit error rate (BER) characteristics at 1 Gbps for each wireless carrier frequency, respectively. Two different word length, $n = 23$ and $n = 31$ are chosen to measure the quality and performance of the wireless link system at different distances.

The eye patterns are measured using a BERTWave MP2100. As can be seen in Fig. 3(a), the eye of the received signal is clearly open, even at the maximum distance allowed by the guide rail system. The time variation at zero crossing is below 188 ps and the eye opening 752 ps. This can also be observed by the BER measurement, achieving an error free transmission with a BER $< 10^{-11}$ (both for 2^{23}-1 and 2^{31}-1) at 1 Gbps and a distance less than 15 cm, as shown in Fig. 3(b). However, for distances between 15 cm and 24 cm, we have obtained a BER $< 10^{-9}$ (both for 2^{23}-1 and 2^{31}-1), being still a good result of the performance of the wireless link system at 101 GHz carrier frequency. For distances in the meter or even kilometer range, additional RF amplifiers would be required as the system performance gets noise limited for such distances. In this receiver scheme, SNR of the system is mostly determined by the noise figure (NF) of set of amplifiers connected after the SBD detector. From Fig. 4(a) and Fig. 4(b), we can observe that the eye pattern at distances larger than 9 cm begin to contract vertically becoming smaller in the center of the eye and as result the BER measurement value is increased. However, the Bit Error Rate (BER) was below 10^{-9} measured using a 2^{23}-1 and 2^{31}-1 PRBS sequence at 1 Gbps and ¿ 9 cm distance between Tx and Rx using an 114 GHz carrier frequency.

The wireless link system is limited by the UTC-PD's bandwidth and the responsivity of the whole antenna-integrated SBD including the silicon lens. Therefore, it gives as result a great difference between Fig. 3(b) and Fig. 4(b). The BER measurement can be improved adding a trans-impedance amplifier in order to saturate the received signal from the output of the second LNA.

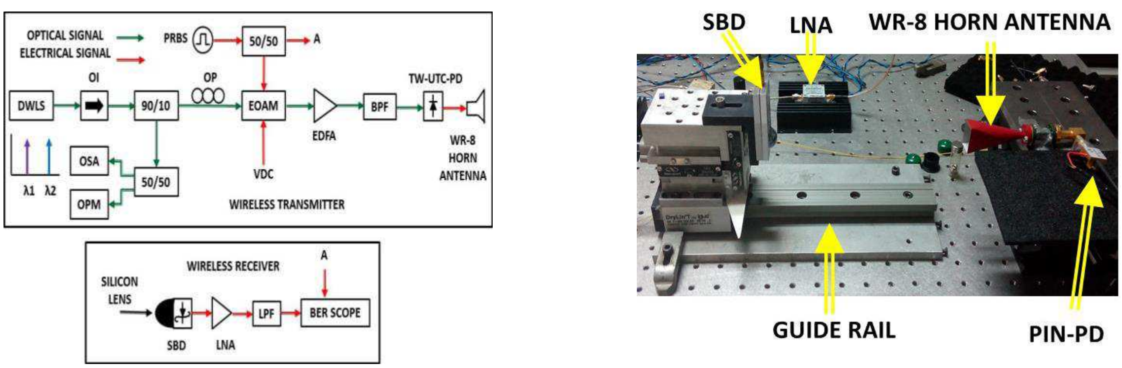

(a) (b)

Figure 2: (a) Block diagram of experimental setup used for F-Band (90–140 GHz) Wireless Link Communication System based on OOK modulation and direct data detection. Data is modulated using an amplitude modulator (EOAM) and amplified using Erbium-doped fiber amplifiers (EDFA). A high speed photodiode launches the electric signal. (b) Photograph of the wireless link measurement setup. A guide rail system is used for moving the receiver away from the transmitter, from 0 cm to 24 cm.

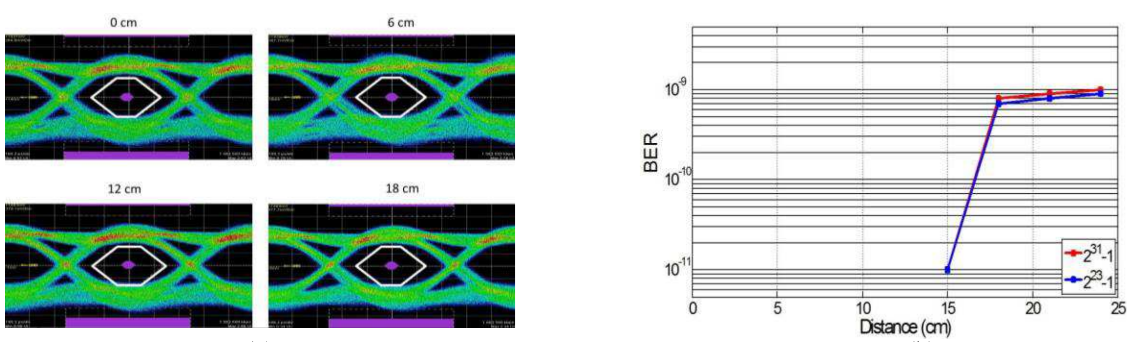

(a) (b)

Figure 3: (a) Eye-Pattern of the received PRBS data, $n = 31$, at 1 Gbps after the transmission of the wireless link. The wireless receiver is placed at different distance from the transmitter, as shown in Fig. 2(b). The carrier frequency is about 101 GHz using a non-return zero digital (NRZ) signal. (b) Bit Error Rate (BER) against distance between the transmitter and the receiver. Two different word length, $n = 23$ and $n = 31$ are selected in order to measure the quality and performance of the wireless link system at different distances.

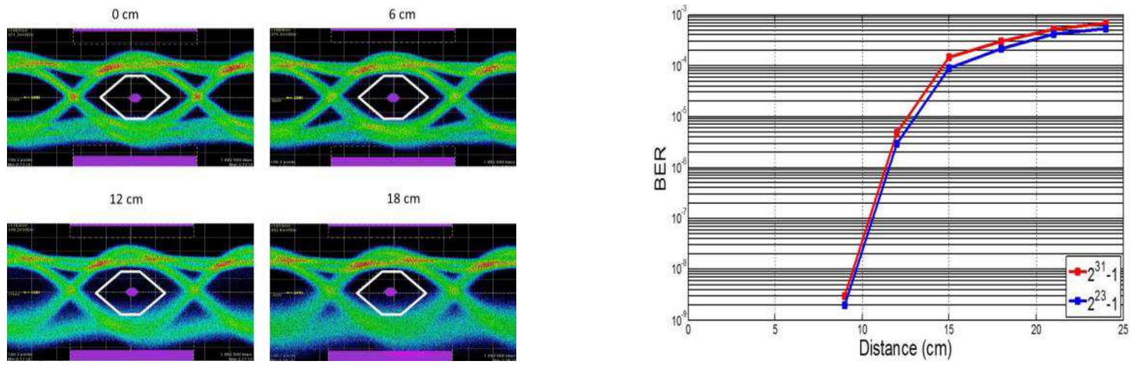

(a) (b)

Figure 4: (a) Eye-Pattern of the received PRBS data, $n = 31$, at 1 Gbps after the transmission of the wireless link. The wireless receiver is placed at different distance from the transmitter, as shown in Fig. 2(b). The carrier frequency is about 114 GHz using a non-return zero digital (NRZ) signal. (b) Bit Error Rate (BER) against distance between the transmitter and the receiver. Two different word length, $n = 23$ and $n = 31$ are selected in order to measure the quality and performance of the wireless link system at different distance.

4. CONCLUSIONS

We have also demonstrated 'error-free' transmission over a photonic enabled wireless link at a data rate of 1 Gbps with BER $< 10^{-11}$ and 10^{-9} over 15 cm and 9 cm distance without observing an error floor (i.e., distance can be extended if RF amplification is provided) using carrier frequencies of 101 GHz and 114 GHz, respectively. The system uses two key components, a PIN-PD and a zero-bias Schottky barrier diode receiver. Both have a great potential to realise compact transmitter and receiver modules. These devices was produced on an InP-based technology multi-project wafer run, with great potential to develop low-cost and compact sources and with the possibility to integrate further functionality.

ACKNOWLEDGMENT

This work was supported by Spanish Ministerio de Economia y Competitividad DiDACTIC project (TEC2013-47753-C3-3-R) and Consejera de Educacin, Juventud y Deporte of Comunidad de Madrid DIFRAGEOS project (P2013/ICE-3004).

REFERENCES

1. Kukutsu, N. and Y. Kado, "Overview of millimeter and terahertz wave application research," *NTT Technical Review*, Vol. 7, No. 3, March 2009.
2. Nagatsuma, T. and H. Ito, "High-power RF uni-traveling-carrier photodiodes (UTC-PDs) and their applications," *Advances in Photodiodes*, Prof. Gian Franco Dalla Betta (Ed.), ISBN: 978-953-307-163-3, InTech, DOI: 10.5772/14800, 2011.
3. Nagatsuma, T., et al., "Photonic generation of millimeter and terahertz waves and its applications," *Applied Electromagnetics and Communications*, Vol. 1, No. 4, 24–26, 2007.
4. Seed, A. J., H. Shams, M. J. Fice, and C. C. Renaud, "TeraHertz photonics for wireless communications," *Journal of Lightwave Technology*, Vol. 33, No. 3, 579–587, 2015.
5. Carpintero, G., K. Balakier, Z. Yang, R.C. Guzmán, A. Corradi, A. Jimenez, G. Kervella, M. J. Fice, M. Lamponi, M. Chitoui, F. van Dijk, C. C. Renaud, A. Wonfor, E. A. J. M. Bente, R. V. Penty, I. H. White, and A. J. Seeds, "Microwave photonic integrated circuits for millimeter-wave wireless communications," *Journal of Lightwave Technology*, Vol. 32, No. 20, 3495–3501, 2014.
6. Smit, M., X. Leijtens, E. Bente, J. Van der Tol, H. Ambrosius, D. Robbins, M. Wale, N. Grote, and M. Schell, "Generic foundry model for InP-based photonics," *IET Optoelectronics*, Vol. 187, 2011.
7. Xu, L., X. J. M. Leijtens, et al., "MMI-reflector: A novel on-chip reflector for photonic integrated circuits," *ECOC Proceedings Vienna '09*, September 2009.